Journal of Ceramic Processing Research. Vol. 23, No. 1, pp. 22~28 (2022)
(Received 28 April 2021, Received in revised form 9 August 2021, Accepted 25 September 2021)
https://doi.org/10.36410/jcpr.2022.23.1.22

J O U R N A L O F
Ceramic Processing Research

Preparation and characterization of hydroxyapatite from portunus sanguinolentus crab shell

J. Rohan[a,*], D. Thenmuhil[b], R. Umapriya[c] and D. Varatharajan[c]
[a]*Adhiyamaan College of Engineering, Hosur, Tamilnadu, India*
[b]*AC TECH campus, Anna University, Chennai, Tamilnadu, India*
[c]*Erode Sengunthar Engineering College, Erode, Tamilnadu, India*

Hydroxyapatite a bio-ceramic is one of the main compounds present in our body tissues. Generally, bones have a high calcium content and Arthritis, Fracture, Infection, Tumours are the main factors that affect bones directly. Presently, steel plates are used in bone replacement surgeries. Natural hydroxyapatite and bones have similar physical and chemical characteristics and this thus makes it biocompatible. Hydroxyapatite can be synthetically derived from crab shells, eggshells and fishbone. Amongst them, crab shells have a high calcium content and as a huge amount of crab shells are produced daily, the same is easily available. Additionally, the cost of crab shells is less and hence, the shells can be used effectively for deriving hydroxyapatite (HA) powder synthetically. A huge quantity of Poryunus Sanguinolentus crab shells is available in and around Rameshwaram coastal area. In this investigation, the Poryunus Sanguinolentus crab shell is used for HA preparation. The reactions between Poryunus Sanguinolentus crab shell powder ($C_8H_{13}05_N$) and calcium pyrophosphate ($Ca_2P_2O_7$) were performed through grinding, followed by the heat treatment to produce Hydroxy Apatite (HA). Further, the physical and chemical characteristics of the HA were analysed and the results derived from the Scanning Electron Microscope (SEM) micrograph, Energy Dispersive X-Ray Analysis (EDAX), X-Ray Diffraction (XRD) analysis and Fourier Transform Infrared Spectroscopy analysis (FTIR), Biocompatibility analysis, Compressive strength and Tensile strength analysis had shown that hence HA can be produced from Poryunus Sanguinolentus crab shells. These results show that the HA powder derived from the shells can be used as a biocompatible material.

Keywords: Crab shell, Hydroxyapatite, Grinding, Heat treatment, Characterization analysis.

Introduction

Crab shells are one of the major natural wastes present in our environment. These shells contain calcium carbonate predominantly in their composition, which makes them a vital component in the preparation of hydroxyapatite (HA) powder. HA powders are predominantly used in the fields of Biomedical and wastewater treatment. Presently, Fractured or infected bones are replaced with the help of steel and they can react with body fluids at conditions of 37 ºC temperature and 7.4 pH level. The implant procedure and the failure in this mechanism are the major reasons behind the extension of research on bioglass preparation and ceramic material is seen as a suitable alternative. Bio ceramics are most preferred for bone preparation, considering their high resistance to corrosion, good compressive strength, low density and low weight.

Hydroxyapatite and Ca-Phosphates are the ceramics used in bone regeneration, modification and attachment. Hydroxyapatite comes with preferred qualities of Bone-bonding and bone growth ability. It also has a similar crystallographic structure and provides perfect biocompatibility with bone. On the other hand, Calcium phosphate ceramic also plays a major role in bone replacement, with its Composition similarity, good bioactivity and osteoconductivity

Hydroxyapatite ($Ca_{10}(PO_4)_6(OH)_2$, HA) acts as catalyst support for chemical reactions [1]. and synthetic Hydroxyapatite is used in various medical applications for replacing bones and teeth [2]. The human body's natural apatite contains carbonate and trace elements [3]. Precursors and processing conditions are the key factors on which the properties of the HA are dependent [4]. Synthesis techniques to prepare HA are sol-gel, hydrothermal technique, aqueous precipitation and solid-state reactions. Generally, Fishbones, eggshells and crab shells are used in the preparation of HA.

Lemos et al. [5] explain the transformation of natural aragonite from the bones of cuttlefish into HA by heat treatment at 200 ºC. Ooi et al. [6] used bovine bone for porous HA synthesis. He also used the heat treatment with a 400-1,200 ºC temperature range. Wu et al. [7] derived the Hydroxyapatite from oyster shells. He took oyster shells powder and calcium pyrophosphate ($Ca_2P_2O_7$) and he also carried out the trial with oyster

*Corresponding author:
Tel : +9994608327
E-mail: rohanchemical@hotmail.com

shell and dicalcium pyrophosphate dihydrate ($CaHPO_4 \cdot 2H_2O$). He used ball milling followed by heat treatment.

However, for this study, outer shells of Poryunus Sanguinolentus crabs are taken. A huge amount of Poryunus Sanguinolentus crab shells are found as a waste from the seafood and the food factory. Nowadays, commercial HAs are relatively expensive. Therefore in this study, crab shells were preferred as the raw materials to minimize the cost and to utilize the waste crab shells. The factors of Crystallinity, Functional identification and composition were determined and discussed.

Materials Involved

In this work, Portunus Sanguinolentus crab shells were collected from the coastal area of Rameshwaram. These shells were cleansed in pure water using a brush, plenty of times until the impurities are removed and followed by the sonication of the 60s. After cleansing, they were dried with air and stored as shown in Fig. 1. Di-Calcium Phosphate Dihydrate (DCPD) was received from Sigma Aldrich. Gelatin was received from Sigma Aldrich. At 50 ^oC, 5 g of gelatin was dissolved in 12 mL of water.

Methodology

Preparation of hydroxyapatite

The powder made from the Portunus Sanguinolentus crab shells was crushed and grounded in an agate mortar. After grinding, it was sieved with a 325-mesh sieve and stored as shown in Fig. 2. Calcium pyrophosphate was prepared by heat-treating of DCPD at 1,000 ^oC for 3 hrs. It was again sieved with a 325-mesh sieve before actual use. This crab shell powder was then mixed with calcium pyrophosphate homogeneously using deionized water in a container as shown in Fig. 3 for the synthesis of HA. In this study, 4:2(S1), 4:3(S2), 4:4(S3) in mole ratio (i.e., the stoichiometric Ca/P content in the composition of hydroxyapatite Ca/P = 1.67) of crab shell powders to calcium pyrophosphate

Fig. 1. Dried Portunus Sanguinolentus crab shell .

Fig. 2. Grinded Portunus Sanguinolentus crab shell powder.

Fig. 3. Homogeneous mixture of Calcium pyrophosphate and Portunus Sanguinolentus crab shell powder.

mixtures were prepared. Samples were grounded through wet milling for 1, 5, and 8 h at a rotating speed of 170 rpm. After milling, the samples were dried completely at 150 ºC (hot air oven) for one day. Further, these powders were heat-treated at a 10 ºC/min rate and maintained at 1,000 ºC temperature for 3hrs durations in independent experiments. Finally, the HA powder was put into various tests to find their character.

Characterization of hydroxyapatite

Scanning Electron Microscope (SEM) with Energy Dispersive X-Ray Analysis (EDAX)

The morphology of the HA powder was studied using SEM with EDAX (S-3000H; HITACHI make). Its formation, size and shape were identified by using the SEM analysis. However, the elemental composition of the HA powder was identified by using the EDAX analysis.

X-Ray Diffraction test (XRD)

XRD (XRD 6000; SHIMADZU make) was used to find the average bulk composition of HA powder. This test is to find the crystallinity by comparing the integrated intensity of the background pattern to that of the sharp peaks.

Fourier Transform Infra-Red Spectroscopy (FTIR) test

HA powder samples were given to the FTIR (IR Prestige-21 model; SHIMADZU make) for the functional group identification.

Compressive strength and Tensile Strength Analysis

6 mL of gelatin solution and 10 g of HA were mixed well to attain a paste. To determine its compressive strength, a 1.5 cm diameter cylindrical shape was prepared by using a glass tube. The samples were dried for 2 h followed by curing at 80 ºC for 12 h. Finally, the compressive strength and Tensile strength of the samples was measured by using Universal Testing Machine (Made: TECHINC.Ltd, Chennai).

Blood compatibility analysis

A hemolysis study with healthy human blood was performed to evaluate the biocompatibility of the HA powder.

Results and Discussion

Scanning electron microscopy analysis

The SEM micrographs of the samples (S1, S2 and S3) show the surface morphology of the samples as shown in Fig. 4. The micrograph was taken with a low magnification of 3 μm as well as the high magnification. These micrographs clearly show that the hydroxyapatite is in crystal form and particles are formed in nano size. These particles attained will thus be effective in bone-forming as its size in all three ratios is approximately equal.

The elemental composition of samples S1, S2 and S3 are shown in Table 2. This result shows that the presence of Ca and P is high for the S1 sample (4:4) and it is reduced in S2 (4:3) and S3 (4:2) samples. This result concluded that the addition of calcium pyrophosphate with HA powder gives the high content of Ca and P in sample S1.

X-Ray diffraction pattern result

All the samples were characterized by using XRD. Fig. 5 shows the XRD pattern of S1, S2 and S3. Ahmed and Ahsan 2008 confirmed the presence of hydroxyapatite with strong diffraction peaks at 31.6, 32.04 and 32.7 and a strong peak at 29·3 for $CaCO_3$. In this study also, the presence of crystalline structure is found from the result of XRD analysis. The diffraction peaks were observed at 26º, 32º, 39º, 37.7º, 40º and 47º as shown in Fig. 5. These peaks correspond to the (002), (211), (212), (310) and (312) planes, which confirms the existence of calcite and HA in the S3 sample (4:4 molar ratio) [8]. Moreover, the calcite peak

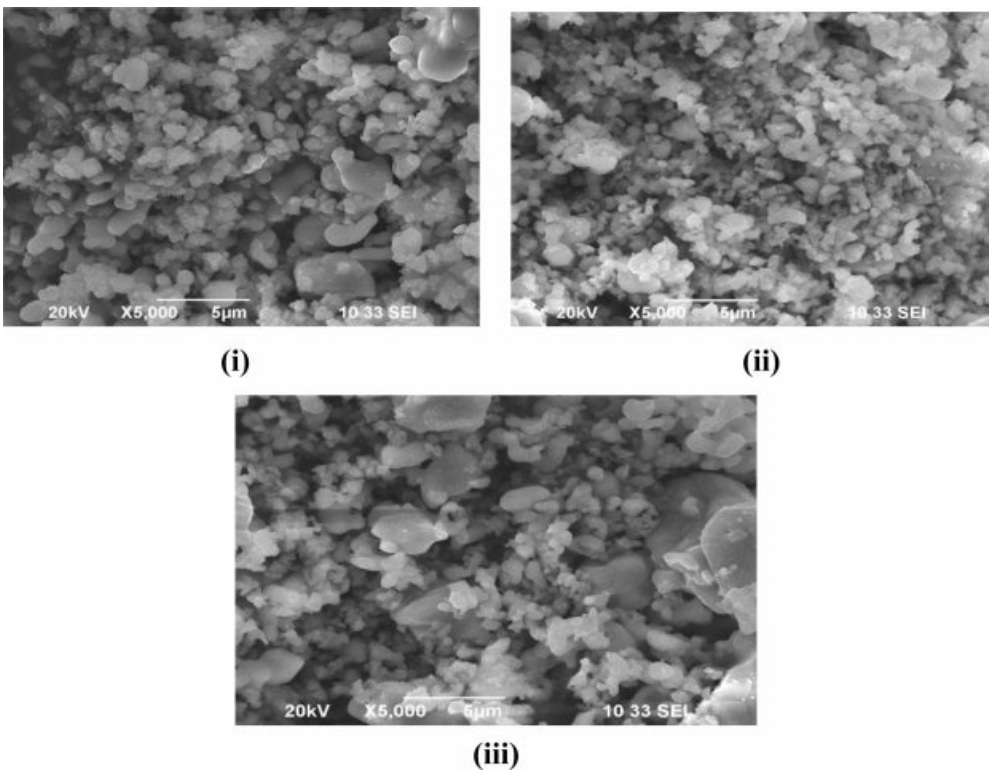

Fig. 4. SEM micrographs of hydroxyapatite (i) 4:4(S1), (ii) 4:3(S2), (iii) 4:2(S3) (mole ratios).

Table 1. Average crystallite size of the Hydroxyapatite samples

Sample Name	FWHM	Crystallite size D, nm
S1	0.5	17.26
S2	0.7	12.32
S3	0.6539	13.21

Table 2. Elemental composition of the Hydroxyapatite powder

Sample Name	Ca (at.%)	O (at.%)	P (at.%)
S1	18.62	65.31	16.07
S2	17.18	69.62	13.20
S3	15.76	72.18	12.06

positions of 37.7° and 40° were significantly decreased with molar ratio variation of Ca/P (4:3 and 4:2). Reduction of calcium pyrophosphate facilitated the formation of Hap can arrive from this. The peaks were recorded at 26°, 32° and 48° corresponding to the (002), (211) and (312) planes, which shows Hap was formed.

The crystallite size of the calcined powder was measured using Scherer's equation, $D = 0.9\lambda/FWHM \cos\theta$; where D is the crystallite diameter in Å, λ the X-ray (CuKα) wavelength in Å(1.5406), θ the diffraction angle in degrees and FWHM (in radian) the half-width measured for the XRD peak. In this study, the highest diffraction peak was chosen for the calculation of crystallite size. Table 1 shows the crystallite size of the products. The average crystallite size of the Hap is 17.26 nm, 12.32 nm and 13.21 nm for S1, S2 and S3 respectively which is similar to the crystallite size of natural bone.

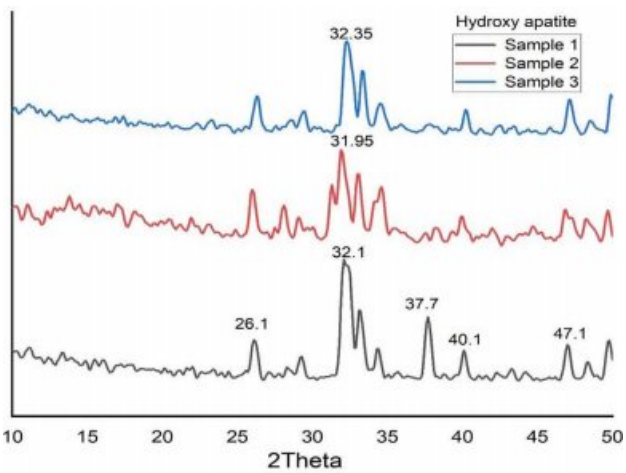

Fig. 5. XRD pattern of Hydroxyapatite (i) 4:4(S1), (ii) 4:3(S2), (iii) 4:2(S3) (mole ratios).

Fourier transform infrared spectroscopy pattern

The FTIR pattern of three different ratios of hydroxyapatite 4:4(S1), 4:3(S2), 4:2(S3) (mole ratios) is shown in Fig. 6. The FTIR spectrum of S1, S2 and S3 shows the absorption bands of carbonate at 1,404.18 cm^{-1}, 1,419.61 cm^{-1}, and 1,411.89 cm^{-1} respectively. This result confirms the $CaCO_3$ presence in the HA powder.

FTIR spectrum shows peaks at 1,049.81 cm^{-1}, 1,026.13

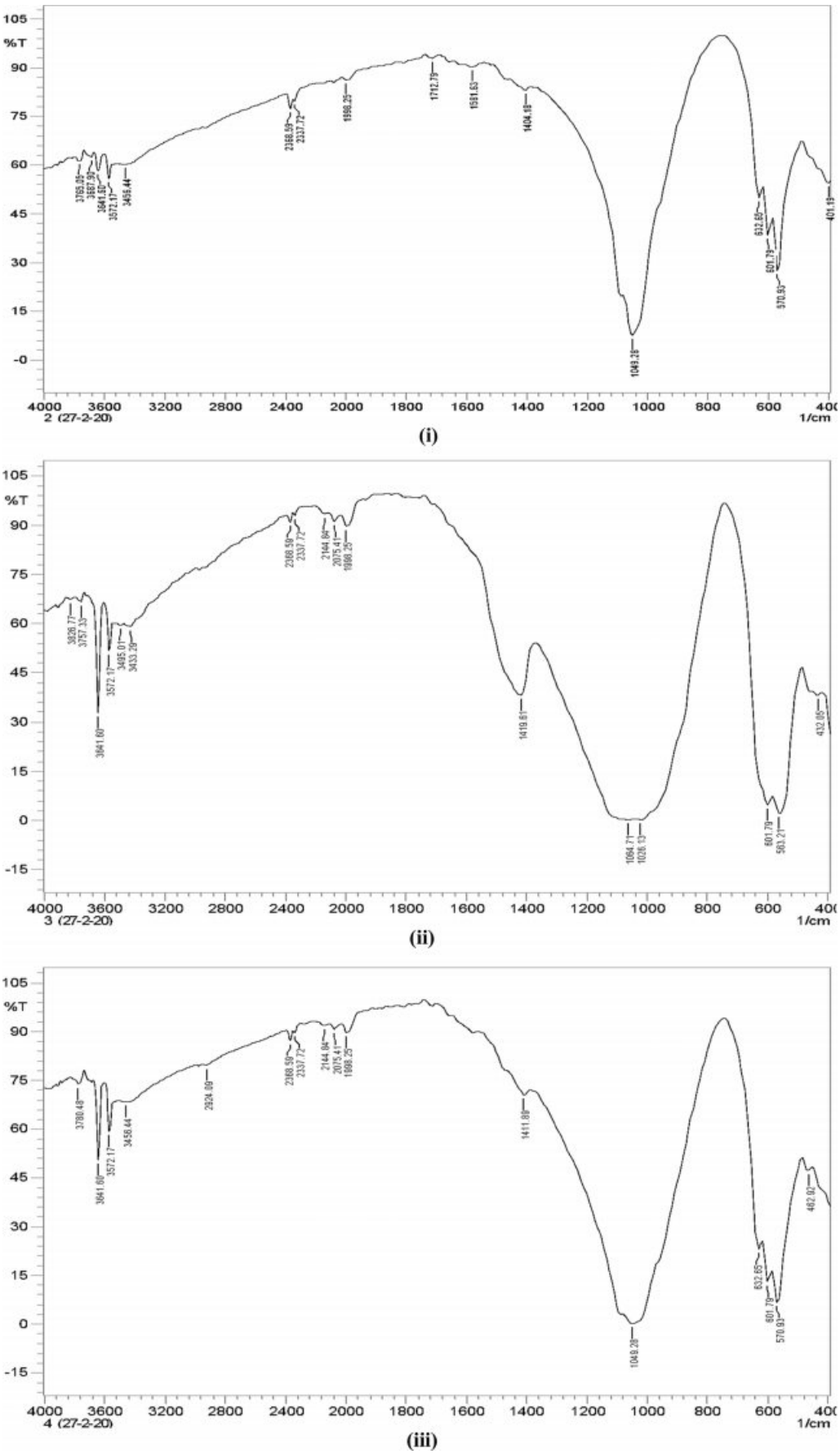

Fig. 6. FTIR Pattern of Hydroxyapatite (i) 4:4(S1), (ii) 4:3(S2), (iii) 4:2(S3) (mole ratios).

Table 3. FTIR band and its corresponding functional groups of Hydroxyapatite powder

Band positions (cm^{-1})			Functional groups
S1	S2	S3	
401.19	432.06	432.92	$V_2 PO_4^{3-}$ bend
570.93	563.21	570.98	$V_4 PO_4^{3-}$ bend
601.79	601.79	601.79	$V_4 PO_4^{3-}$ bend
1,049.28	1,026.13	1,049.28	$V_3 PO_4^{3-}$ stretch
1,404.18	1,419.61	1,411.89	CO_3^{2-} bend
3,455.44	3,433.29	3,455.44	OH^- stretch

Table 4. Compressive strength and Tensile Strength of Hydroxyapatite samples

Sample Name	Tensile strength (MPa)	Compressive strength (MPa)
S1	35	5.0
S2	34	4.9
S3	32	4.7

cm^{-1} and 1,049.28 cm^{-1} for S1, S2 and S3 samples respectively. It represents the presence of the crystallized apatite phase. The peak at 1,049.81 cm^{-1}, 1,026.13 cm^{-1} and 1,049.28 cm^{-1} represents the v_3 vibration mode of phosphate groups. The sharp peaks from 570 to 602 cm^{-1} indicate the bending mode of phosphate. FTIR band positions and corresponding assignments are tabulated in Table 3. IR spectrum of HA is similar to that of Ahmed and Ahsan 2008 study report. This spectrum mentioning that the inorganic materials are formed in this particle composition.

Earlier reports mentioned the two classes of carbonate substitutions on HA. One is A-type and another one is B-type [9]. The carbonates are substituted at the site of O–H vibrations in A-type and phosphate substitution can be taken place in the vibrational sites. Hence, the band at 1,049 cm^{-1} shows that the B-type are formed. This can be highly used in biomedical applications.

Compressible strength and tensile strength analysis

Compressive strength and tensile strength of the samples S1, S2 and S3 are determined and obtained result is tabulated in Table 4. The compressive strength and tensile strength depend on particle size, percentage of moisture and nature of adhesives. S1(4:4) has the highest tensile strength and compressive strength compared with S2 and S3. This compressive strength is less compared to the compressive strength of natural bone (165 MPa). Hence, the prepared HA can be used in the defects of low weight-bearing bones like the spinal cord bone.

Blood comapatability analysis

The haemolytic behaviour of the HA powder was investigated at various concentrations as shown in Fig 7. The obtained results were compared to the American

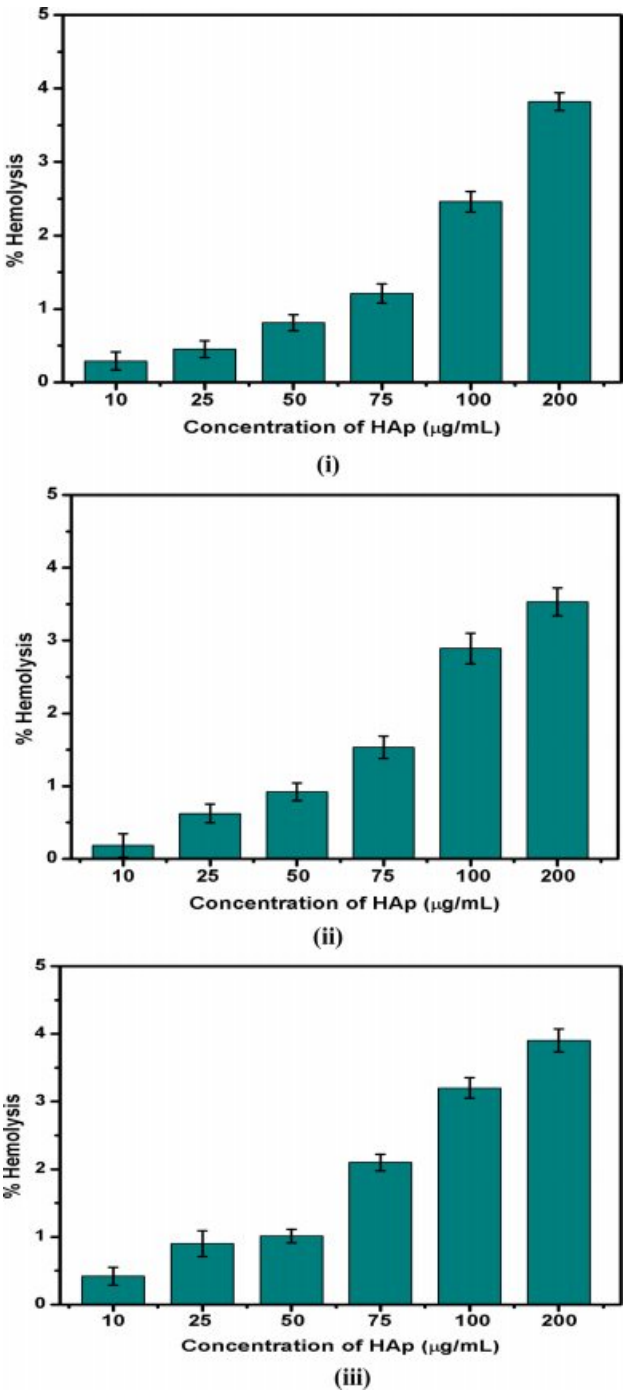

Fig. 7. Haemolytic behaviour of Hydroxyapatite samples (i) 4:4(S1), (ii) 4:3(S2), (iii) 4:2(S3) (mole ratios).

Society standards. Up to 75 µg/mL addition of HA exhibited 2% haemolysis, which shows the non-haemolytic and non-toxic behaviour of the samples. All three samples show a haemolysis percentage from 2.5% to 3.8% with 100 to 200 µg/mL concentration of HA powder, which indicates that the haemolytic behaviour was slightly increased with the increase in HA powder. This haemolytic activity can be attributed to higher concentrations of introducing HA along with the blood cells.

Conclusion

This work explains the synthesis of hydroxyapatite from Poryunus Sanguinolentus crab shell powder mixed with Calcium Pyrophosphate by ball milling and through heat treatment. The XRD pattern of the S1 (4:4) milled sample showed a good amount of HA phase. For the composition ratio of 4:3 and 4:2, the HA concentration was decreased while lowering the composition ratio. This variation results in a high quantity HA phase. The FTIR results of the samples showed the OH^{-}, $PO4^{3-}$ bonds and thus concluded that crystals of hydroxyapatite were formed for all three samples. The average crystallite sizes of the Hap are 17.26 nm, 12.32 nm and 13.21 nm for S1, S2 and S3 respectively which is similar to the crystallite size of natural bone. Additionally, the blood compatibility of the three samples is also good. The compressible strength and tensile strength of the S1 are higher as compared to S2 and S3. The composition ratio thus plays an important role in particle size, mechanical strength, biocompatibility, crystal and functional group formation. Therefore going forward, this work can be carried out for bone replacement in vivo and in vitro study.

References

1. R.Z. Le Geros, Clin. Orthop. Relat. Res. 395 (2002) 81-98.
2. K. De Groot, Ceram. Int. 19[5] (1993) 363-366.
3. A. John, H.K. Varma, T.V. Kumari, J. Biomater. Appl. 18 (2003) 63-78.
4. H.S. Liu, T.S. Chin, L.S. Lai, S.Y. Chiu, K.H. Chung, C.S. Chang, and M.T. Lui, Ceram. Int. 23 (1997) 19-25.
5. P. Shuk, W. Suchanek, T. Hao, E. Gulliver, R.E. Riman, M. Senna, K.S. Tenhuisen, and V.F. Janas, J. Mater. Res. 16[5] (2001) 1231-1234.
6. K.J.L. Burg, S. Porter, F. Kellam. Biomaterials. 21[23] (2000) 2347-2359.
7. S.-C. Wu, H.-C. Hsu, S.-K. Hsu, C.-P. Tseng, and W.-F. Ho, Advanced Powder Technology, 28[4] (2017) 1154-1158.
8. J.H.G Rocha, A.F. Lemos, S. Agathopoulos, P. Valério, S. Kannan, and J.M.F. Ferreira, J.M.F. Bone. 37 (2005) 850-857.
9. J.H. McElhaney, J.L. Fogle, J.W. Melvin, R.R. Haynes, V.L. Roberts, and N.M. Alem, J. Biomech. 3[5] (1970) 495-511.
10. S. Ahmed, F. Nigar, A.I. Mustafa, and M. Ahsan, Transactions of the Indian Ceramic Society, 76[4] (2017) 215-221.
11. Y. Tanaka, Y. Hirata, and R. Yoshinaka, Journal of Ceramic Processing Research, 4[4] (2003) 197-201.